AIMS Mathematics, 9(10): 28058–28078.
DOI: 10.3934/math.20241361
Received: 08 August 2024
Revised: 30 August 2024
Accepted: 09 September 2024
Published: 27 September 2024

http://www.aimspress.com/journal/Math

Research article

Optical fractals and Hump soliton structures in integrable Kuralay-II system

Azzh Saad Alshehry[1], **Safyan Mukhtar**[2,3,*] **and Ali M. Mahnashi**[4]

[1] Department of Mathematical Sciences, Faculty of Sciences, Princess Nourah Bint Abdulrahman University, P.O. Box 84428, Riyadh 11671, Saudi Arabia
[2] Department of Basic Sciences, General Administration of Preparatory Year, King Faisal University, P.O. Box 400, Al Ahsa 31982, Saudi Arabia
[3] Department of Mathematics and Statistics, College of Science, King Faisal University, P.O. Box 400, Al Ahsa 31982, Saudi Arabia
[4] Department of Mathematics, Faculty of Science, Jazan University, P.O. Box 2097, Jazan 45142, Kingdom of Saudi Arabia

* **Correspondence:** Email: smahmad@kfu.edu.sa.

Abstract: The integrable Kuralay-II system (K-IIS) plays a significant role in discovering unique complex nonlinear wave phenomena that are particularly useful in optics. This system enhances our understanding of the intricate dynamics involved in wave interactions, solitons, and nonlinear effects in optical phenomena. Using the Riccati modified extended simple equation method (RMESEM), the primary objective of this research project was to analytically find and analyze a wide range of new soliton solutions, particularly fractal soliton solutions, in trigonometric, exponential, rational, hyperbolic, and rational-hyperbolic expressions for K-IIS. Some of these solutions displayed a combination of contour, two-dimensional, and three-dimensional visualizations. This clearly demonstrates that the generated solitons solutions are fractals due to the instability produced by periodic-axial perturbation in complex solutions. In contrast, the genuine solutions, within the framework of K-IIS, take the form of hump solitons. This work demonstrates the adaptability of the K-IIS for studying intricate nonlinear phenomena in a wide range of scientific and practical disciplines. The results of this work will eventually significantly influence our comprehension and analysis of nonlinear wave dynamics in related physical systems.

Keywords: nonlinear partial differential equations; integrable Kuralay-II system; Riccati modified extended simple equation method; optical fractals; Hump solitons; Periodic-Axial perturbation
Mathematics Subject Classification: 34G20, 35A20, 35A22, 35R11

1. Introduction

This study begins by setting the targeted model in the context of its earlier research and thoroughly analyzing pertinent literature. This part provides an overview of the study's main goals, identifies gaps in the existing literature, and includes information on the manuscript's organizational structure.

Nonlinear partial differential equations (NPDEs) have become increasingly prominent as fundamental study fields in recent decades. This is particularly true for discovering new characteristics of intricate phenomena in various scientific domains, such as atomic, particle, optical, nuclear, and biological physics [1–3]. To demonstrate various engineering, physics, and natural processes, several nonlinear models have been developed [4, 5]. Several methods and strategies have been developed to investigate numerical, analytical, and semi-analytical solutions. Spline methods [6], finite difference method [7], the Adomian decomposition method [8], the variational iteration method [9], finite eliminating method [10], the $(\frac{G'}{G})$-expansion method [11], the Riccati expansion method [12], the sine-cosine expansion method [13], the tanh-expansion method [14], the modified simple equation method [15], and the sech-tanh expansion method [16]. Over the last couple of years, analysis of nonlinear dynamic systems and soliton has attracted much interest because of its broad applications in areas as diverse as optics and fluid mechanics and material sciences [17, 18]. Analytical solutions of nonlinear differential equations including generalized systems, algebraic constraints, and different fractional, and perturbation models has often been found to capture the physical behavior as the wave, the fluid, and the electromagnetic vibrations [19, 20]. To obtain more information, one used exact solutions and methods such as Bäcklund transformation, bifurcation analysis, and observer design in these systems. This paper extends the current literature by emphasizing the improvement of solutions? accuracy and versatility in different mathematical and natural science problems through the use of sophisticated mathematical tools, namely fuzzy logic and fractional calculus [21–23]. We hope that by applying these techniques in conjunction with existing approaches, enhanced models are created that enable better analysis and decision-making in situations characterized by risk and ambiguity [24, 25].

It is important to investigate explicit solutions for NPDEs using analytical techniques, and it is crucial to comprehend the behaviors of several elements in various scientific fields [26–28]. Soliton solutions, among the explicit solutions to NPDEs, remain significant from an academic perspective because they offer more breadth and depth than conventional solutions. A soliton is a single, autonomous wave packet that moves across a medium without altering its shape or velocity [29–31]. They are valuable in many technological and scientific fields because they have inherent stability and longevity. They provide effective information transport and far-reaching coherence preservation for nonlinear systems. To obtain novel soliton solution outcomes, mathematicians have created powerful methods. Among these noteworthy techniques are the Khater methods [32], Sin-Gordon method [33], Poincaré-Lighthill-Kuo method [34], exp-function method [35], $(\frac{G'}{G})$-expansion method [36, 37], Kudryashov method [38], Riccati-Bernoulli Sub-ODE [39], Sardar sub-equation method [40], sub-equation method [41], extended direct algebraic method (EDAM) [42–45], and Hirota's bilinear method [46]. These incredibly efficient techniques, aimed at creating soliton solutions for NPDEs, are constantly evolving. They are a critical development designed to produce new analytical solutions for NPDEs. Traveling wave patterns inside NPDEs are of great interest in many fields, such as physics, fluid mechanics, and engineering and other scientific fields [47–51].

In modern mathematics and physics, gauge equivalence is used for relating some integrable

nonlinear evolution equations (NEEs) to each other or, in fact, in a quite different manner. It is known that the nonlinear Schrödinger equation is the gauge partner of the Heisenberg ferromagnetic equation. Gauge equivalencies allow us to exploit the relationship between integrable nonlinear equations. Using these equivalencies, we can obtain crucial insights into each equation from its gauge partner. This is achieved by transforming solutions from one equation into solutions from another [52–54]. In a formal approach, the system may be represented by two equivalent zero curvature criteria, corresponding to two different sets of Lax operators [55, 56]. This connection has been thoroughly examined in the previously cited literature and other pertinent sources. This characteristic of the gauge transformation has been investigated to build the gauge equivalent counterpart of the Zhaidary equation and to derive integrable reductions and generalizations. The Zhaidary equations allow for several integrable reductions, including the integrable Kuralay-II system (K-IIS), Shynaray-II and Zhanbota-II. Among these, the K-IIS, found in [57–59], has been considered in this research. This model is articulated as:

$$\begin{aligned} &ip_t - p_{xt} - qp = 0, \\ &q_x - 2\mu(|p|^2)_t = 0, \end{aligned} \tag{1.1}$$

where $i = \sqrt{-1}$, $q = q(x,t)$ as a real valued function and $p = p(x,t)$ as a complex valued function, x and t are real spatiotemporal variables, and $\mu = \pm 1$. This model has applications in many different disciplines of optics and physics.

Numerous other researchers have addressed K-IIS in integer and fractional form with different mathematical tools before this research survey. For instance, by employing the Hirota bilinear approach, Sagidullayeva et al. [57] investigated this model in 2022 and determined a gauge equivalency between them. Faridi et al. [58] employed the innovative approach of auxiliary equations to analyze the integrable motion of induced space curves and deduce various soliton solutions. To look at exact solutions of the K-IIS, such as solitary waves and optical solitons, Mathanaranjan [59] used the new extended auxiliary equation and modified F-expansion approaches. Furthermore, the modulation instability gain spectrum was obtained by applying linear stability analysis to modulation instability analysis. Exact solutions of the fractional K-IIS were investigated by Zafar et al. [60] in 2023 using a variety of techniques, including the extended sinh-Gordon equation expansion, the generalized Kudryashov, and exp-function schemes. Using the Jacobi elliptic function expansion approach, Khan et al. [61] looked into the precise solitary wave solutions to the truncated fractional K-IISs. These investigations' soliton solutions have potential uses in the scientific and technical domains.

Previous studies on the exploration of the solitonic phenomena in K-IIS by numerous investigators make it evident that optical fractal solutions have not yet been investigated. This claim highlights a substantial gap in the existing corpus of research. Our paper seeks to address this gap by offering a thorough analysis of the model and outlining the suggested technique: the Riccati modified extended simple equation method (RMESEM).

This study's goals and objectives are as follows. The intended K-IIS will first be transformed into a single, more manageable nonlinear ordinary differential equation (NODE) via a wave transformation. Next, we will convert the NODE into an algebraic system of equations by assuming a closed form solution using the RMESEM technique. Ultimately, the system will be examined using the Maple tool to determine the K-IIS optical soliton solutions. In conclusion, we will analyze how temporal variation and free parameters affect the model's optical soliton solutions, illustrating a few of these solutions with a combination of contour, two-, and three-dimensional visualizations. Additionally, we

will demonstrate how the instability caused by periodic-axial perturbation in complex solutions results in derived solitons solutions that resemble fractals, while real solutions, as defined by K-IIS, resemble hump solitons.

The remaining sections are organized as follows. The analytical processes of the RMESEM are explained in Section 2. K-IIS is addressed and discussed in Section 3 to generate novel optical soliton solutions. A graphic depiction of the propagating behavior of the generated optical solitons is given in Section 4. The results are outlined in Section 5, and the final section includes the appendix.

2. The functional strategy of Riccati modified extended simple equation method (RMESEM)

In order to study soliton phenomena in nonlinear models, numerous analytical approaches have been established in the literature. The functioning process of the upgraded RMESEM is described in this section. Examining the resulting generic NPDE [62]:

$$A(\mathfrak{p}, \mathfrak{p}_t, \mathfrak{p}_{y_1}, \mathfrak{p}_{y_2}, \mathfrak{p}\mathfrak{p}_{y_1}, \ldots) = 0, \tag{2.1}$$

where $\mathfrak{p} = \mathfrak{p}(t, y_1, y_2, y_3, \ldots, y_r)$.

The procedures listed below will be followed in order to solve (2.1):

(1) The variable-form complex transformation $\mathfrak{p}(t, y_1, y_2, y_3, \ldots, y_r) = \mathfrak{P}(\varrho)$ is first performed. For ϱ, several representations are known. By useing this technique, Eq (2.1) is transformed to get the subsequent NODE:

$$B(\mathfrak{P}, \mathfrak{P}'\mathfrak{P}, \mathfrak{P}', \ldots) = 0, \tag{2.2}$$

where $\mathfrak{P}' = \frac{d\mathfrak{P}}{d\varrho}$. The homogeneous balance condition (2.2) may be on occasion enforced on the NODE with the use of the integrating equation.

(2) Next, utilizing the solution provided by the extended Riccati-NODE, the resulting finite series-based solution for the NODE in (2.2) is recommended:

$$\mathfrak{P}(\varrho) = \sum_{j=0}^{s} F_j \left(\frac{B'(\varrho)}{B(\varrho)}\right)^j + \sum_{j=0}^{s-1} S_j \left(\frac{B'(\varrho)}{B(\varrho)}\right)^j \cdot \left(\frac{1}{B(\varrho)}\right). \tag{2.3}$$

Here, the solution to the resultant extended Riccati-NODE is denoted by $B(\varrho)$, and the unidentified constants required to be found later are represented by the variables $F_j(j = 0, ..., s)$ and $S_j(j = 0, ..., s-1)$.

$$B'(\varrho) = \lambda + \eta B(\varrho) + \nu(B(\varrho))^2, \tag{2.4}$$

where λ, η and ν are constants.

(3) We may get the positive integer s needed in Eq (2.3) by homogeneously balancing the greatest nonlinear component and the highest-order derivative in Eq (2.2).

(4) All the components of $B(\varrho)$ are then combined into an equal ordering when (2.3) is inserted into (2.2) or the equation that emerges from the integration of (2.2). When this process is used, an equation in terms of $B(\varrho)$ is generated. By setting the coefficients in the resulting equation to zero, one may get an algebraic system of equations representing the variables $F_j(j = 0, ..., s)$ and $S_j(j = 0, ..., s-1)$ along with additional accompanying parameters.

(5) With Maple, the set of nonlinear algebraic equations is analytically evaluated.

(6) To acquire analytical soliton solutions for (2.1), the next step is to compute and enter the unidentified values in addition to $B(\varrho)$ (the Eq (2.4) solution) in Eq (2.3). By using (2.4)'s general solution, we might potentially derive a multitude of soliton solutions.

Following is an illustration of these clusters.

3. Execution of RMESEM and construction of optical soliton solutions

In this study, we present optical soliton solutions for Eq (2.1) by utilizing the suggested RMESEM. We start with the complex wave transformation that follows:

$$\begin{aligned} &p(x,t) = e^{\theta i}W(\varrho), \quad q(x,t) = Q(\varrho), \\ &\varrho = \varsigma x + \delta t, \quad \theta = \alpha x + \beta t. \end{aligned} \tag{3.1}$$

After replacing (3.1) in (2.1) and partitioning the imaginary and real parts, we get:

$$\begin{aligned} &(\delta - \alpha\delta - \beta\varsigma)iP' - \delta\varsigma P'' + (\alpha\beta - Q - \beta)P = 0, \\ &\varsigma Q' - 4\mu\delta PP' = 0, \quad P = P(\varrho), \quad Q = Q(\varrho). \end{aligned} \tag{3.2}$$

One time integration w.r.t ϱ of the second part in (3.2) with zero constant of integration yields:

$$Q = \frac{2\mu\delta P^2}{\varsigma}. \tag{3.3}$$

Putting (3.3) in (3.2) reduces the real part of the entire system to the ensuing single NODE:

$$(\alpha - 1)\beta P - \varsigma\delta P'' - \frac{2\mu\delta P^3}{\varsigma} = 0, \tag{3.4}$$

with the constraint condition from the imaginary part:

$$\alpha = \frac{\delta - \beta\varsigma}{\delta}. \tag{3.5}$$

Using (3.4) to determine the homogeneous balancing principle within $-\varsigma\delta P''$ and $-\frac{2\mu\delta P^3}{\varsigma}$, $s = 1$ is recommended. Inputting $s = 1$ into (2.3) yields the following series solution for Eq (3.4):

$$P(\varrho) = \sum_{j=0}^{1} F_j \left(\frac{B'(\varrho)}{B(\varrho)}\right)^j + S_0\left(\frac{1}{B(\varrho)}\right). \tag{3.6}$$

By inserting (3.6) into (3.4) and collecting every single term with the same ordering of $B(\varrho)$, an expression in $B(\varrho)$ is obtained. By setting the coefficients to zero, the statement is simplified to a system of nonlinear algebraic equations. Using Maple to solve the resulting problem, the following three types of solutions are found:

Case 1.

$$F_0 = \frac{1}{2}\frac{S_0\eta}{\lambda}, F_1 = 0, S_0 = S_0, \beta = \frac{1}{2}\sqrt{2\eta^2 - 8\lambda\nu}\delta, \delta = \delta, \varsigma = \frac{\sqrt{-\mu}S_0}{\lambda}. \tag{3.7}$$

Case 2.

$$F_0 = -\frac{1}{2}F_1\eta, F_1 = F_1, S_0 = -F_1\lambda, \beta = \frac{1}{2}\sqrt{2\eta^2 - 8\lambda\nu}\delta, \delta = \delta, \varsigma = \sqrt{-\mu}F_1. \tag{3.8}$$

Assuming Case 1, we acquire the subsequent clumps of optical soliton solutions for K-IIS stated in (1.1):

Clump 1.1. In the case of $N < 0,\ \nu \neq 0$,

$$\begin{aligned} p_{1,1}(t,x) &= e^{i\theta}\Bigg(\frac{1}{2}\frac{S_0\eta}{\lambda} + S_0\left(-\frac{1}{2}\frac{\eta}{\nu} + \frac{1}{2}\frac{\sqrt{-N}\tan\left(\frac{1}{2}\sqrt{-N}\varrho\right)}{\nu}\right)^{-1}\Bigg), \\ q_{1,1}(t,x) &= \frac{2\mu\delta}{\varsigma}\Bigg(\frac{1}{2}\frac{S_0\eta}{\lambda} + S_0\left(-\frac{1}{2}\frac{\eta}{\nu} + \frac{1}{2}\frac{\sqrt{-N}\tan\left(\frac{1}{2}\sqrt{-N}\varrho\right)}{\nu}\right)^{-1}\Bigg)^2, \end{aligned} \tag{3.9}$$

$$\begin{aligned} p_{1,2}(t,x) &= e^{i\theta}\Bigg(\frac{1}{2}\frac{S_0\eta}{\lambda} + S_0\left(-\frac{1}{2}\frac{\eta}{\nu} - \frac{1}{2}\frac{\sqrt{-N}\cot\left(\frac{1}{2}\sqrt{-N}\varrho\right)}{\nu}\right)^{-1}\Bigg), \\ q_{1,2}(t,x) &= \frac{2\mu\delta}{\varsigma}\Bigg(\frac{1}{2}\frac{S_0\eta}{\lambda} + S_0\left(-\frac{1}{2}\frac{\eta}{\nu} - \frac{1}{2}\frac{\sqrt{-N}\cot\left(\frac{1}{2}\sqrt{-N}\varrho\right)}{\nu}\right)^{-1}\Bigg)^2, \end{aligned} \tag{3.10}$$

$$\begin{aligned} p_{1,3}(t,x) &= e^{i\theta}\Bigg(\frac{1}{2}\frac{S_0\eta}{\lambda} + S_0\left(-\frac{1}{2}\frac{\eta}{\nu} + \frac{1}{2}\frac{\sqrt{-N}\left(\tan\left(\sqrt{-N}\varrho\right) + \sec\left(\sqrt{-N}\varrho\right)\right)}{\nu}\right)^{-1}\Bigg), \\ q_{1,3}(t,x) &= \frac{2\mu\delta}{\varsigma}\Bigg(\frac{1}{2}\frac{S_0\eta}{\lambda} + S_0\left(-\frac{1}{2}\frac{\eta}{\nu} + \frac{1}{2}\frac{\sqrt{-N}\left(\tan\left(\sqrt{-N}\varrho\right) + \sec\left(\sqrt{-N}\varrho\right)\right)}{\nu}\right)^{-1}\Bigg)^2, \end{aligned} \tag{3.11}$$

and

$$\begin{aligned} p_{1,4}(t,x) &= e^{i\theta}\Bigg(\frac{1}{2}\frac{S_0\eta}{\lambda} + S_0\left(-\frac{1}{2}\frac{\eta}{\nu} + \frac{1}{2}\frac{\sqrt{-N}\left(\tan\left(\sqrt{-N}\varrho\right) - \sec\left(\sqrt{-N}\varrho\right)\right)}{\nu}\right)^{-1}\Bigg), \\ q_{1,4}(t,x) &= \frac{2\mu\delta}{\varsigma}\Bigg(\frac{1}{2}\frac{S_0\eta}{\lambda} + S_0\left(-\frac{1}{2}\frac{\eta}{\nu} + \frac{1}{2}\frac{\sqrt{-N}\left(\tan\left(\sqrt{-N}\varrho\right) - \sec\left(\sqrt{-N}\varrho\right)\right)}{\nu}\right)^{-1}\Bigg)^2. \end{aligned} \tag{3.12}$$

Clump 1.2. In the case of $N > 0,\ \nu \neq 0$,

$$\begin{aligned} p_{1,5}(t,x) &= e^{i\theta}\Bigg(\frac{1}{2}\frac{S_0\eta}{\lambda} + S_0\left(-\frac{1}{2}\frac{\eta}{\nu} - \frac{1}{2}\frac{\sqrt{N}\tanh\left(\frac{1}{2}\sqrt{N}\varrho\right)}{\nu}\right)^{-1}\Bigg), \\ q_{1,5}(t,x) &= \frac{2\mu\delta}{\varsigma}\Bigg(\frac{1}{2}\frac{S_0\eta}{\lambda} + S_0\left(-\frac{1}{2}\frac{\eta}{\nu} - \frac{1}{2}\frac{\sqrt{N}\tanh\left(\frac{1}{2}\sqrt{N}\varrho\right)}{\nu}\right)^{-1}\Bigg)^2, \end{aligned} \tag{3.13}$$

$$
\begin{aligned}
p_{1,6}(t,x) &= e^{i\theta}\Bigg(\frac{1}{2}\,\frac{S_0\eta}{\lambda}+S_0\Bigg(-\frac{1}{2}\,\frac{\eta}{\nu}-\frac{1}{2}\,\frac{\sqrt{N}\left(\tanh\left(\sqrt{N}\varrho\right)+i\mathrm{sech}\left(\sqrt{N}\varrho\right)\right)}{\nu}\Bigg)^{-1}\Bigg),\\
q_{1,6}(t,x) &= \frac{2\mu\,\delta}{\varsigma}\Bigg(\frac{1}{2}\,\frac{S_0\eta}{\lambda}+S_0\Bigg(-\frac{1}{2}\,\frac{\eta}{\nu}-\frac{1}{2}\,\frac{\sqrt{N}\left(\tanh\left(\sqrt{N}\varrho\right)+i\mathrm{sech}\left(\sqrt{N}\varrho\right)\right)}{\nu}\Bigg)^{-1}\Bigg)^{2},
\end{aligned}
\tag{3.14}
$$

$$
\begin{aligned}
p_{1,7}(t,x) &= e^{i\theta}\Bigg(\frac{1}{2}\,\frac{S_0\eta}{\lambda}+S_0\Bigg(-\frac{1}{2}\,\frac{\eta}{\nu}-\frac{1}{2}\,\frac{\sqrt{N}\left(\tanh\left(\sqrt{N}\varrho\right)-i\mathrm{sech}\left(\sqrt{N}\varrho\right)\right)}{\nu}\Bigg)^{-1}\Bigg),\\
q_{1,7}(t,x) &= \frac{2\mu\,\delta}{\varsigma}\Bigg(\frac{1}{2}\,\frac{S_0\eta}{\lambda}+S_0\Bigg(-\frac{1}{2}\,\frac{\eta}{\nu}-\frac{1}{2}\,\frac{\sqrt{N}\left(\tanh\left(\sqrt{N}\varrho\right)-i\mathrm{sech}\left(\sqrt{N}\varrho\right)\right)}{\nu}\Bigg)^{-1}\Bigg)^{2},
\end{aligned}
\tag{3.15}
$$

and

$$
\begin{aligned}
p_{1,8}(t,x) &= e^{i\theta}\Bigg(\frac{1}{2}\,\frac{S_0\eta}{\lambda}+S_0\Bigg(-\frac{1}{2}\,\frac{\eta}{\nu}-\frac{1}{4}\,\frac{\sqrt{N}\left(\tanh\left(\frac{1}{4}\,\sqrt{N}\varrho\right)-\coth\left(\frac{1}{4}\,\sqrt{N}\varrho\right)\right)}{\nu}\Bigg)^{-1}\Bigg),\\
q_{1,8}(t,x) &= \frac{2\mu\,\delta}{\varsigma}\Bigg(\frac{1}{2}\,\frac{S_0\eta}{\lambda}+S_0\Bigg(-\frac{1}{2}\,\frac{\eta}{\nu}-\frac{1}{4}\,\frac{\sqrt{N}\left(\tanh\left(\frac{1}{4}\,\sqrt{N}\varrho\right)-\coth\left(\frac{1}{4}\,\sqrt{N}\varrho\right)\right)}{\nu}\Bigg)^{-1}\Bigg)^{2}.
\end{aligned}
\tag{3.16}
$$

Clump 1.3. In the case of $N = 0,\ \eta \neq 0$,

$$
\begin{aligned}
p_{1,9}(t,x) &= e^{i\theta}\Bigg(\frac{1}{2}\,\frac{S_0\eta}{\lambda}-\frac{1}{2}\,\frac{S_0\eta^2\varrho}{\lambda\,(\eta\varrho+2)}\Bigg),\\
q_{1,9}(t,x) &= \frac{2\mu\,\delta}{\varsigma}\Bigg(\frac{1}{2}\,\frac{S_0\eta}{\lambda}-\frac{1}{2}\,\frac{S_0\eta^2\varrho}{\lambda\,(\eta\varrho+2)}\Bigg)^{2}.
\end{aligned}
\tag{3.17}
$$

Clump 1.4. In the case of $N = 0$, in case when $\eta = \nu = 0$,

$$
\begin{aligned}
p_{1,10}(t,x) &= e^{i\theta}\Bigg(\frac{S_0}{\lambda\varrho}\Bigg),\\
q_{1,10}(t,x) &= \frac{2\mu\,\delta}{\varsigma}\Bigg(\frac{S_0}{\lambda\varrho}\Bigg)^{2}.
\end{aligned}
\tag{3.18}
$$

Clump 1.5. In the case of $\eta = \varpi$, $\lambda = h\varpi(h \neq 0)$ and $\nu = 0$,

$$
\begin{aligned}
p_{1,11}(t,x) &= e^{i\theta}\Bigg(\frac{1}{2}\,\frac{S_0}{h}+\frac{S_0}{\mathrm{e}^{\varpi\varrho}-h}\Bigg),\\
q_{1,11}(t,x) &= \frac{2\mu\,\delta}{\varsigma}\Bigg(\frac{1}{2}\,\frac{S_0}{h}+\frac{S_0}{\mathrm{e}^{\varpi\varrho}-h}\Bigg)^{2}.
\end{aligned}
\tag{3.19}
$$

In the above optical soliton solutions of Case 1,

$$
\varrho = \left(\frac{\sqrt{-\mu}S_0}{\lambda}\right)x+\delta t,\quad \theta = \left(\frac{\delta-\beta\varsigma}{\delta}\right)x+\left(\frac{1}{2}\,\sqrt{2\,\eta^2-8\,\lambda\,\nu}\delta\right)t.
$$

Assuming Case 2, we acquire the subsequent clumps of optical soliton solutions for K-IIS stated in (1.1):

Clump 2.1. In the case of $N < 0,\ \nu \neq 0$,

$$\begin{aligned}
p_{2,1}(t,x) &= e^{i\theta}\Big(-\frac{1}{2}F_1\eta - \frac{1}{2}\frac{F_1N\left(1+\left(\tan\left(\frac{1}{2}\sqrt{-N}\varrho\right)\right)^2\right)}{-\eta+\sqrt{-N}\tan\left(\frac{1}{2}\sqrt{-N}\varrho\right)} - \frac{F_1\lambda}{\left(-\frac{1}{2}\frac{\eta}{\nu}+\frac{1}{2}\frac{\sqrt{-N}\tan\left(\frac{1}{2}\sqrt{-N}\varrho\right)}{\nu}\right)}\Big),\\
q_{2,1}(t,x) &= \frac{2\mu\,\delta}{\varsigma}\Big(-\frac{1}{2}F_1\eta - \frac{1}{2}\frac{F_1N\left(1+\left(\tan\left(\frac{1}{2}\sqrt{-N}\varrho\right)\right)^2\right)}{-\eta+\sqrt{-N}\tan\left(\frac{1}{2}\sqrt{-N}\varrho\right)} - \frac{F_1\lambda}{\left(-\frac{1}{2}\frac{\eta}{\nu}+\frac{1}{2}\frac{\sqrt{-N}\tan\left(\frac{1}{2}\sqrt{-N}\varrho\right)}{\nu}\right)}\Big)^2,
\end{aligned} \tag{3.20}$$

$$\begin{aligned}
p_{2,2}(t,x) &= e^{i\theta}\Big(-\frac{1}{2}F_1\eta + \frac{1}{2}\frac{F_1N\left(1+\left(\cot\left(\frac{1}{2}\sqrt{-N}\varrho\right)\right)^2\right)}{\eta+\sqrt{-N}\cot\left(\frac{1}{2}\sqrt{-N}\varrho\right)} - \frac{F_1\lambda}{\left(-\frac{1}{2}\frac{\eta}{\nu}-\frac{1}{2}\frac{\sqrt{-N}\cot\left(\frac{1}{2}\sqrt{-N}\varrho\right)}{\nu}\right)}\Big),\\
q_{2,2}(t,x) &= \frac{2\mu\,\delta}{\varsigma}\Big(-\frac{1}{2}F_1\eta + \frac{1}{2}\frac{F_1N\left(1+\left(\cot\left(\frac{1}{2}\sqrt{-N}\varrho\right)\right)^2\right)}{\eta+\sqrt{-N}\cot\left(\frac{1}{2}\sqrt{-N}\varrho\right)} - \frac{F_1\lambda}{\left(-\frac{1}{2}\frac{\eta}{\nu}-\frac{1}{2}\frac{\sqrt{-N}\cot\left(\frac{1}{2}\sqrt{-N}\varrho\right)}{\nu}\right)}\Big)^2,
\end{aligned} \tag{3.21}$$

$$\begin{aligned}
p_{2,3}(t,x) =& e^{i\theta}\Big(-\frac{F_1N\left(1+\sin\left(\sqrt{-N}\varrho\right)\right)}{\cos\left(\sqrt{-N}\varrho\right)\left(-\eta\cos\left(\sqrt{-N}\varrho\right)+\sqrt{-N}\sin\left(\sqrt{-N}\varrho\right)+\sqrt{-N}\right)}\\
&- F_1\lambda\left(-\frac{1}{2}\frac{\eta}{\nu}+\frac{1}{2}\frac{\sqrt{-N}\left(\tan\left(\sqrt{-N}\varrho\right)+\sec\left(\sqrt{-N}\varrho\right)\right)}{\nu}\right)^{-1} - \frac{1}{2}F_1\eta\Big),\\
q_{2,3}(t,x) =& \frac{2\mu\,\delta}{\varsigma}\Big(-\frac{F_1N\left(1+\sin\left(\sqrt{-N}\varrho\right)\right)}{\cos\left(\sqrt{-N}\varrho\right)\left(-\eta\cos\left(\sqrt{-N}\varrho\right)+\sqrt{-N}\sin\left(\sqrt{-N}\varrho\right)+\sqrt{-N}\right)}\\
&- F_1\lambda\left(-\frac{1}{2}\frac{\eta}{\nu}+\frac{1}{2}\frac{\sqrt{-N}\left(\tan\left(\sqrt{-N}\varrho\right)+\sec\left(\sqrt{-N}\varrho\right)\right)}{\nu}\right)^{-1} - \frac{1}{2}F_1\eta\Big)^2,
\end{aligned} \tag{3.22}$$

and

$$\begin{aligned}
p_{2,4}(t,x) =& e^{i\theta}\Big(\frac{F_1N\left(\sin\left(\sqrt{-N}\varrho\right)-1\right)}{\cos\left(\sqrt{-N}\varrho\right)\left(-\eta\cos\left(\sqrt{-N}\varrho\right)+\sqrt{-N}\sin\left(\sqrt{-N}\varrho\right)-\sqrt{-N}\right)}\\
&- F_1\lambda\left(-\frac{1}{2}\frac{\eta}{\nu}+\frac{1}{2}\frac{\sqrt{-N}\left(\tan\left(\sqrt{-N}\varrho\right)-\sec\left(\sqrt{-N}\varrho\right)\right)}{\nu}\right)^{-1} - \frac{1}{2}F_1\eta\Big),\\
q_{2,4}(t,x) =& \frac{2\mu\,\delta}{\varsigma}\Big(\frac{F_1N\left(\sin\left(\sqrt{-N}\varrho\right)-1\right)}{\cos\left(\sqrt{-N}\varrho\right)\left(-\eta\cos\left(\sqrt{-N}\varrho\right)+\sqrt{-N}\sin\left(\sqrt{-N}\varrho\right)-\sqrt{-N}\right)}\\
&- F_1\lambda\left(-\frac{1}{2}\frac{\eta}{\nu}+\frac{1}{2}\frac{\sqrt{-N}\left(\tan\left(\sqrt{-N}\varrho\right)-\sec\left(\sqrt{-N}\varrho\right)\right)}{\nu}\right)^{-1} - \frac{1}{2}F_1\eta\Big)^2.
\end{aligned} \tag{3.23}$$

Clump 2.2. In the case of $N > 0,\ \nu \neq 0$,

$$\begin{aligned} p_{2,5}(t,x) &= e^{i\theta}\Big(-\frac{1}{2}F_1\eta - \frac{1}{2}\frac{F_1N\left(-1+\left(\tanh\left(\frac{1}{2}\sqrt{N}\varrho\right)\right)^2\right)}{\eta+\sqrt{N}\tanh\left(\frac{1}{2}\sqrt{N}\varrho\right)} - \frac{F_1\lambda}{\left(-\frac{1}{2}\frac{\eta}{\nu}-\frac{1}{2}\frac{\sqrt{N}\tanh\left(\frac{1}{2}\sqrt{N}\varrho\right)}{\nu}\right)}\Big), \\ q_{2,5}(t,x) &= \frac{2\mu\delta}{\varsigma}\Big(-\frac{1}{2}F_1\eta - \frac{1}{2}\frac{F_1N\left(-1+\left(\tanh\left(\frac{1}{2}\sqrt{N}\varrho\right)\right)^2\right)}{\eta+\sqrt{N}\tanh\left(\frac{1}{2}\sqrt{N}\varrho\right)} - \frac{F_1\lambda}{\left(-\frac{1}{2}\frac{\eta}{\nu}-\frac{1}{2}\frac{\sqrt{N}\tanh\left(\frac{1}{2}\sqrt{N}\varrho\right)}{\nu}\right)}\Big)^2, \end{aligned} \tag{3.24}$$

$$\begin{aligned} p_{2,6}(t,x) =& e^{i\theta}\Big(-\frac{F_1N\left(-1+i\sinh\left(\sqrt{N}\varrho\right)\right)}{\cosh\left(\sqrt{N}\varrho\right)\left(\eta\cosh\left(\sqrt{N}\varrho\right)+\sqrt{N}\sinh\left(\sqrt{N}\varrho\right)+i\sqrt{N}\right)} \\ & - F_1\lambda\left(-\frac{1}{2}\frac{\eta}{\nu}-\frac{1}{2}\frac{\sqrt{N}\left(\tanh\left(\sqrt{N}\varrho\right)+i\mathrm{sech}\left(\sqrt{N}\varrho\right)\right)}{\nu}\right)^{-1} - \frac{1}{2}F_1\eta\Big), \\ q_{2,6}(t,x) =& \frac{2\mu\delta}{\varsigma}\Big(-\frac{F_1N\left(-1+i\sinh\left(\sqrt{N}\varrho\right)\right)}{\cosh\left(\sqrt{N}\varrho\right)\left(\eta\cosh\left(\sqrt{N}\varrho\right)+\sqrt{N}\sinh\left(\sqrt{N}\varrho\right)+i\sqrt{N}\right)} \\ & - F_1\lambda\left(-\frac{1}{2}\frac{\eta}{\nu}-\frac{1}{2}\frac{\sqrt{N}\left(\tanh\left(\sqrt{N}\varrho\right)+i\mathrm{sech}\left(\sqrt{N}\varrho\right)\right)}{\nu}\right)^{-1} - \frac{1}{2}F_1\eta\Big)^2, \end{aligned} \tag{3.25}$$

$$\begin{aligned} p_{2,7}(t,x) =& e^{i\theta}\Big(-\frac{F_1N\left(1+i\sinh\left(\sqrt{N}\varrho\right)\right)}{\cosh\left(\sqrt{N}\varrho\right)\left(-\eta\cosh\left(\sqrt{N}\varrho\right)-\sqrt{N}\sinh\left(\sqrt{N}\varrho\right)+i\sqrt{N}\right)} \\ & - F_1\lambda\left(-\frac{1}{2}\frac{\eta}{\nu}-\frac{1}{2}\frac{\sqrt{N}\left(\tanh\left(\sqrt{N}\varrho\right)-i\mathrm{sech}\left(\sqrt{N}\varrho\right)\right)}{\nu}\right)^{-1} - \frac{1}{2}F_1\eta\Big), \\ q_{2,7}(t,x) =& \frac{2\mu\delta}{\varsigma}\Big(-\frac{F_1N\left(1+i\sinh\left(\sqrt{N}\varrho\right)\right)}{\cosh\left(\sqrt{N}\varrho\right)\left(-\eta\cosh\left(\sqrt{N}\varrho\right)-\sqrt{N}\sinh\left(\sqrt{N}\varrho\right)+i\sqrt{N}\right)} \\ & - F_1\lambda\left(-\frac{1}{2}\frac{\eta}{\nu}-\frac{1}{2}\frac{\sqrt{N}\left(\tanh\left(\sqrt{N}\varrho\right)-i\mathrm{sech}\left(\sqrt{N}\varrho\right)\right)}{\nu}\right)^{-1} - \frac{1}{2}F_1\eta\Big)^2, \end{aligned} \tag{3.26}$$

and

$$\begin{aligned} p_{2,8}(t,x) =& e^{i\theta}\Big(-\frac{1}{2}F_1\eta - \frac{1}{4}\frac{F_1N\left(2\left(\cosh\left(\frac{1}{4}\sqrt{N}\varrho\right)\right)^2-1\right)}{\xi\left(-2\eta\xi+\sqrt{N}\right)} \\ & - F_1\lambda\left(-\frac{1}{2}\frac{\eta}{\nu}-\frac{1}{4}\frac{\sqrt{N}\left(\tanh\left(\frac{1}{4}\sqrt{N}\varrho\right)-\coth\left(\frac{1}{4}\sqrt{N}\varrho\right)\right)}{\nu}\right)^{-1}\Big), \end{aligned}$$

$$q_{2,8}(t,x) = \frac{2\mu\,\delta}{\varsigma}\Big(-\frac{1}{2}F_1\eta - \frac{1}{4}\frac{F_1 N\left(2\left(\cosh\left(\frac{1}{4}\sqrt{N}\varrho\right)\right)^2-1\right)}{\xi\left(-2\eta\xi+\sqrt{N}\right)} - F_1\lambda\left(-\frac{1}{2}\frac{\eta}{\nu} - \frac{1}{4}\frac{\sqrt{N}\left(\tanh\left(\frac{1}{4}\sqrt{N}\varrho\right)-\coth\left(\frac{1}{4}\sqrt{N}\varrho\right)\right)}{\nu}\right)^{-1}\Big)^2. \tag{3.27}$$

Clump 2.3. In the case of $N = 0,\ \eta \neq 0$,

$$\begin{aligned} p_{2,9}(t,x) &= e^{i\theta}\Big(-\frac{1}{2}F_1\eta - 2\frac{F_1}{\varrho\,(\eta\varrho+2)} + \frac{1}{2}\frac{F_1\eta^2\varrho}{\eta\varrho+2}\Big),\\ q_{2,9}(t,x) &= \frac{2\mu\,\delta}{\varsigma}\Big(-\frac{1}{2}F_1\eta - 2\frac{F_1}{\varrho\,(\eta\varrho+2)} + \frac{1}{2}\frac{F_1\eta^2\varrho}{\eta\varrho+2}\Big)^2. \end{aligned} \tag{3.28}$$

Clump 2.4. In the case of $N = 0$, in case when $\eta = \lambda = 0$,

$$\begin{aligned} p_{2,10}(t,x) &= e^{i\theta}\Big(-\frac{F_1}{\varrho}\Big),\\ q_{2,10}(t,x) &= \frac{2\mu\,\delta}{\varsigma}\Big(-\frac{F_1}{\varrho}\Big)^2. \end{aligned} \tag{3.29}$$

Clump 2.5. In the case of $\eta = \varpi$, $\lambda = h\varpi (h \neq 0)$ and $\nu = 0$,

$$\begin{aligned} p_{2,11}(t,x) &= e^{i\theta}\Big(-\frac{1}{2}F_1\varpi + \frac{F_1\varpi\,\mathrm{e}^{\varpi\varrho}}{\mathrm{e}^{\varpi\varrho}-h} - \frac{F_1 h\varpi}{\mathrm{e}^{\varpi\varrho}-h}\Big),\\ q_{2,11}(t,x) &= \frac{2\mu\,\delta}{\varsigma}\Big(-\frac{1}{2}F_1\varpi + \frac{F_1\varpi\,\mathrm{e}^{\varpi\varrho}}{\mathrm{e}^{\varpi\varrho}-h} - \frac{F_1 h\varpi}{\mathrm{e}^{\varpi\varrho}-h}\Big)^2. \end{aligned} \tag{3.30}$$

Clump 2.6. In the case of $\eta = \varpi$, $\nu = h\varpi (h \neq 0)$ and $\lambda = 0$,

$$\begin{aligned} p_{2,12}(t,x) &= e^{i\theta}\Big(-\frac{1}{2}F_1\varpi - \frac{F_1\varpi}{-1+h\mathrm{e}^{\varpi\varrho}}\Big),\\ q_{2,12}(t,x) &= \frac{2\mu\,\delta}{\varsigma}\Big(-\frac{1}{2}F_1\varpi - \frac{F_1\varpi}{-1+h\mathrm{e}^{\varpi\varrho}}\Big)^2. \end{aligned} \tag{3.31}$$

Clump 2.7. In the case of $\lambda = 0$, $\nu \neq 0$ and $\eta \neq 0$,

$$\begin{aligned} p_{2,13}(t,x) &= e^{i\theta}\Big(-\frac{1}{2}F_1\eta + \frac{F_1\eta\,(\sinh(\eta\varrho)-\cosh(\eta\varrho))}{-\cosh(\eta\varrho)+\sinh(\eta\varrho)-b_2}\Big),\\ q_{2,13}(t,x) &= \frac{2\mu\,\delta}{\varsigma}\Big(-\frac{1}{2}F_1\eta + \frac{F_1\eta\,(\sinh(\eta\varrho)-\cosh(\eta\varrho))}{-\cosh(\eta\varrho)+\sinh(\eta\varrho)-b_2}\Big)^2, \end{aligned} \tag{3.32}$$

and

$$\begin{aligned} p_{2,14}(t,x) &= e^{i\theta}\Big(-\frac{1}{2}F_1\eta + \frac{F_1\eta\,b_2}{\cosh(\eta\varrho)+\sinh(\eta\varrho)+b_2}\Big),\\ q_{2,14}(t,x) &= \frac{2\mu\,\delta}{\varsigma}\Big(-\frac{1}{2}F_1\eta + \frac{F_1\eta\,b_2}{\cosh(\eta\varrho)+\sinh(\eta\varrho)+b_2}\Big)^2. \end{aligned} \tag{3.33}$$

In the above optical soliton solutions of Case 2,

$$\varrho = (\sqrt{-\mu}F_1)x + \delta t, \quad \theta = (\frac{\delta - \beta\varsigma}{\delta})x + (\frac{1}{2}\sqrt{2\eta^2 - 8\lambda\nu\delta})t.$$

4. Discussion

In the present section of the study, we provide the frameworks of the several optical wave types that are included in the model. Using RMESEM, we were able to extract and visually represent the wave patterns of optical solitons in 3D, contour, and 2D forms. Comprehending the behavior of related physical events requires these understandings. The discovered optical soliton solutions are predicted to significantly expand our understanding of the dynamics of optical pulse theory in optical fibers. There might be several beneficial uses for these produced optical solitons in the telecom industry. Moreover, our suggested RMESEM illustrates its use by expanding the range of optical soliton solutions, providing significant understanding into the K-IIS dynamics, and indicating potential uses in nonlinear model management.

4.1. The dynamics of p(x,t)

This subsection presents images of a few artificially created optical solitons within the framework of K-IIS complex solutions, (Figures 1–6). The purpose of the images is to provide a visual representation of how these objects lose stability as they get closer to an axis, displaying periodic-axial disturbances and eventually forming optical fractals. In the context of K-IIS, an optical soliton is a self-sustaining pattern that moves across fiber optic medium without altering its form or speed. When these waves interact or collide with other waves of a similar kind, they are well known for their ability for rebuilding and maintaining themselves. However, our investigation revealed that the dispersion of nonlinearity and the presence of external input lead to axial and periodic disturbances in the created solitons, which in turn cause instabilities in the soliton and lead to the production of optical fractals. Nevertheless, the soliton interaction (especially with lumps) and self-resemblance have also contributed to the formation of the fractal structure in some of our solitons.

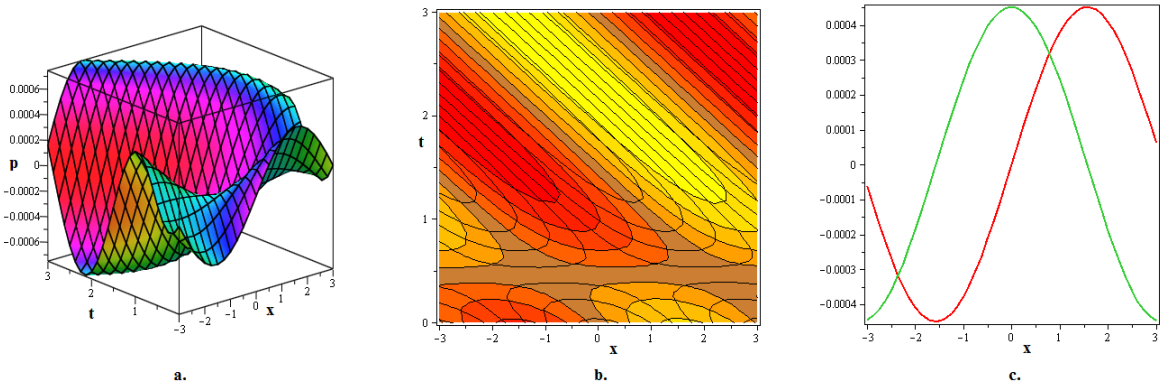

Figure 1. a. 3D graph, b. contour graph, and c. 2D graph representing optical fractal soliton solution $p_{1,5}(t, x)$ articulated in (3.13) for $\lambda := 2, \eta := 5, \nu := 2, S_0 := 0.1E^{-2}, \delta := -1, \mu := -1$.

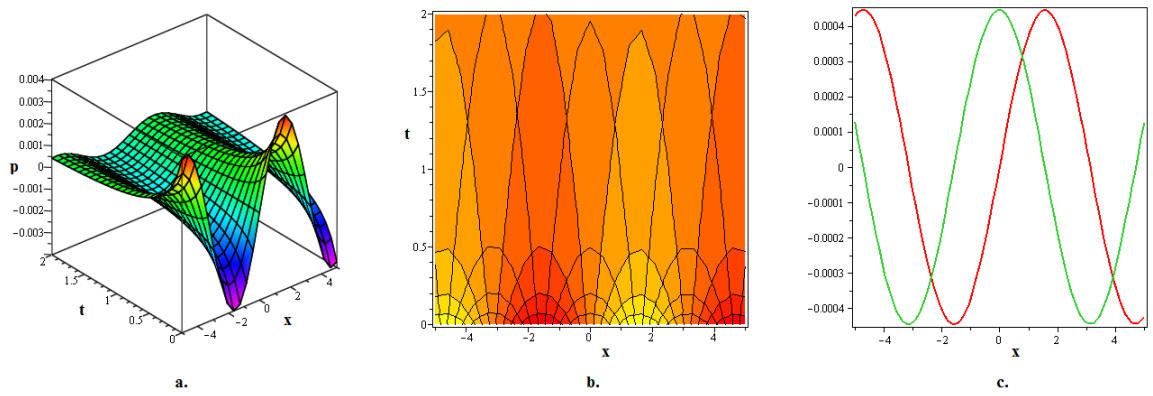

Figure 2. a. 3D graph, b. contour graph, and c. 2D graph representing optical fractal soliton solution $p_{1,9}(t,x)$ articulated in (3.17) for $\lambda := 1, \eta := 4, \nu := 4, S_0 := 0.2E^{-2}, \delta := 2, \mu := -1$.

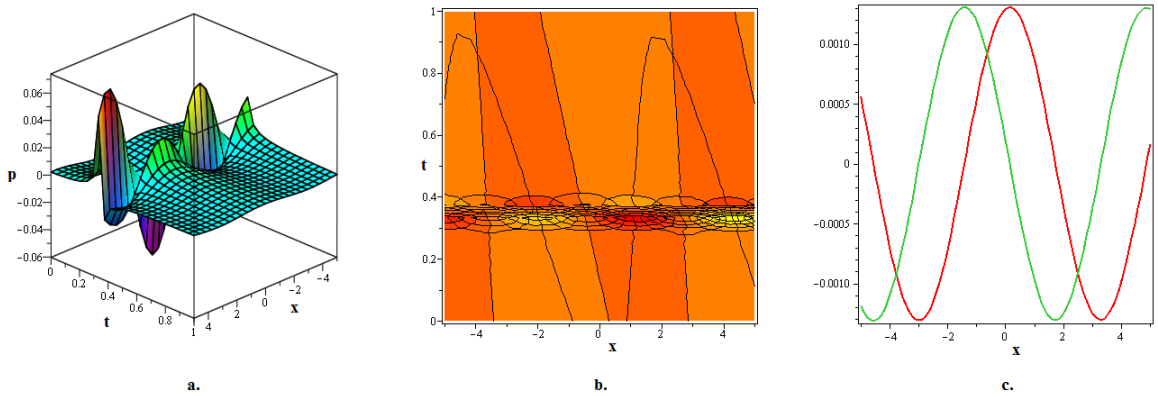

Figure 3. a. 3D graph, b. contour graph, and c. 2D graph representing optical fractal soliton solution $p_{1,11}(t,x)$ articulated in (3.19) for $\lambda := 4, \eta := 2, \nu := 0, \varpi := 2, h := 2, S_0 := 0.3E^{-2}, \delta := 1, \mu := -1$.

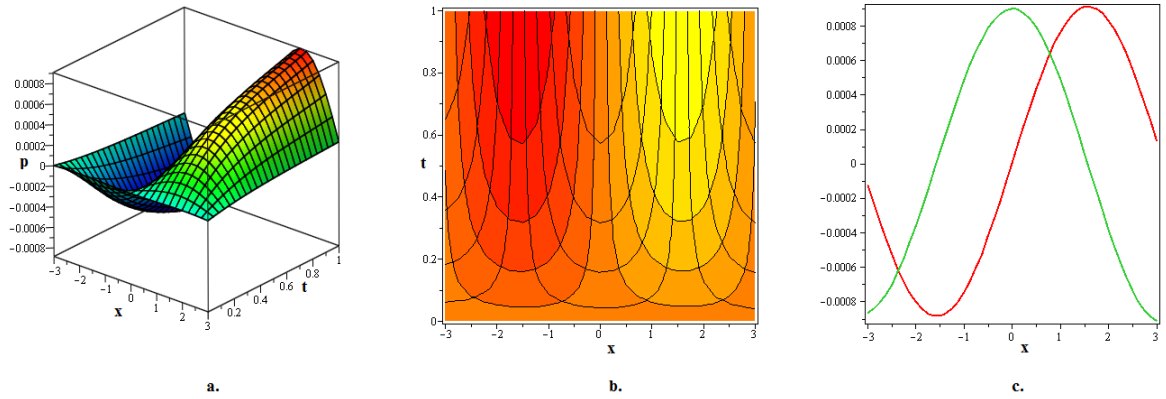

Figure 4. a. 3D graph, b. contour graph, and c. 2D graph representing optical fractal soliton solution $p_{2,1}(t,x)$ articulated in (3.20) for $\lambda := 1, \eta := 1, \nu := 1, F_1 := 0.3E^{-2}, \delta := 1, \mu := -1$.

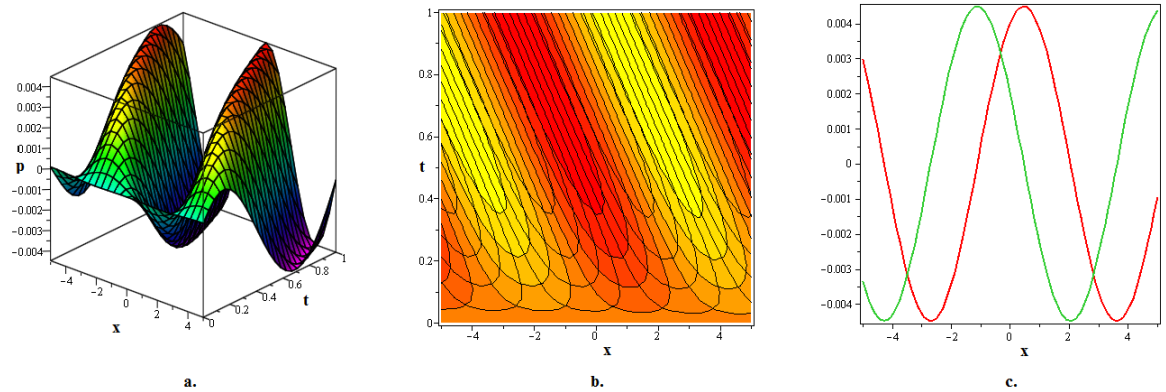

Figure 5. a. 3D graph, b. contour graph, and c. 2D graph representing optical fractal soliton solution $p_{2,5}(t, x)$ articulated in (3.24) for $\lambda := 4, \eta := 10, \nu := 4, F_1 := 0.15E^{-2}, \delta := 1, \mu := -1$.

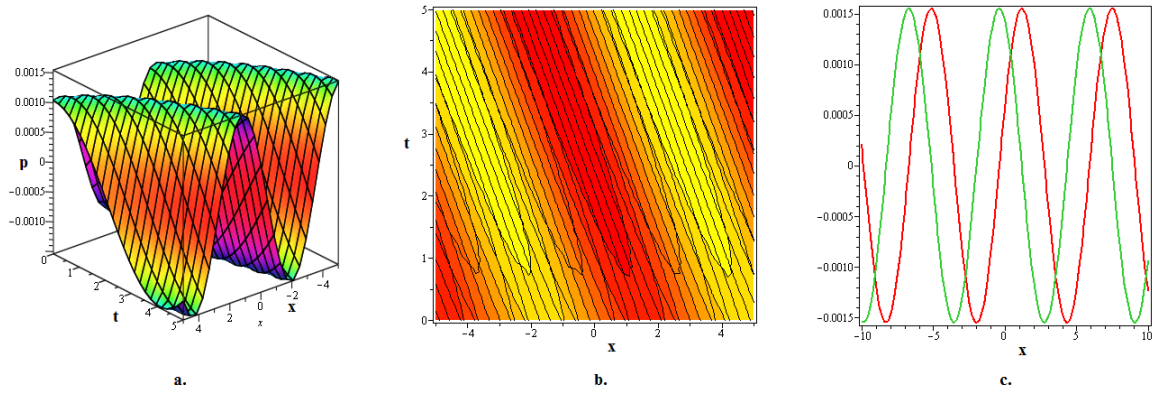

Figure 6. a. 3D graph, b. contour graph, and c. 2D graph representing optical fractal soliton solution $p_{2,13}(t, x)$ articulated in (3.32) for $\lambda := 0, \eta := 1, \nu := 2, F_1 := 0.32E^{-2}, \delta := .5, \mu := -1, b_2 := 5$.

4.2. The dynamics of q(x,t)

In order to illustrate that the real solutions, in the framework of K-IIS, adopt the shape of hump solitons, several developed optical solitons are presented in this subsection, (Figures 7–12). A localized wave packet that keeps its form and speed while moving through a medium is called a hump optical soliton. This unique variety of kink soliton features peaks one or more during light hump and drops during dark hump. These solitons arise in models with modulation instability and are caused by the action of the nonlinear medium. The hump may develop in the presence of disturbances because these wave structures are stable and localized. Hump optical solitons are a vital field of study with many applications in fiber and nonlinear optics, where regulating light propagation plays a key role. The efficiency of optical systems can be improved by the manipulation and generation of such hump optical soliton.

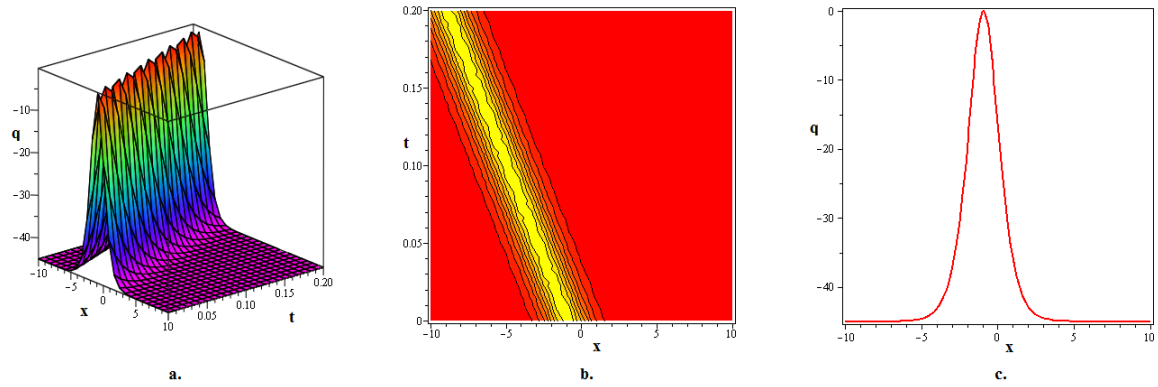

Figure 7. a. 3D graph, b. contour graph, and c. 2D graph representing optical bright-hump soliton solution $q_{1,5}(t,x)$ articulated in (3.13) for $\lambda := 2, \eta := 5, \nu := 2, S_0 := 1, \delta := 20, \mu := -1$.

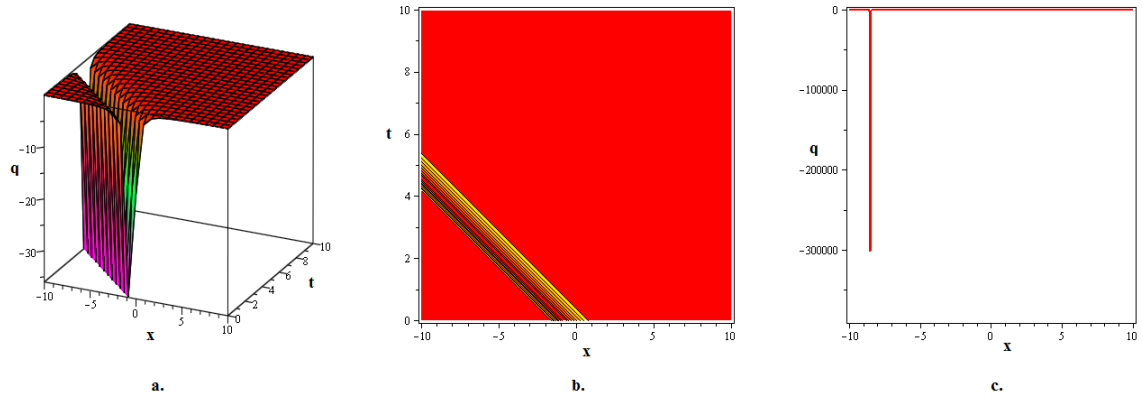

Figure 8. a. 3D graph, b. contour graph, and c. 2D graph representing optical dark-hump soliton solution $q_{1,9}(t,x)$ articulated in (3.17) for $\lambda := 1, \eta := 4, \nu := 4, S_0 := 1, \delta := 2, \mu := -1$.

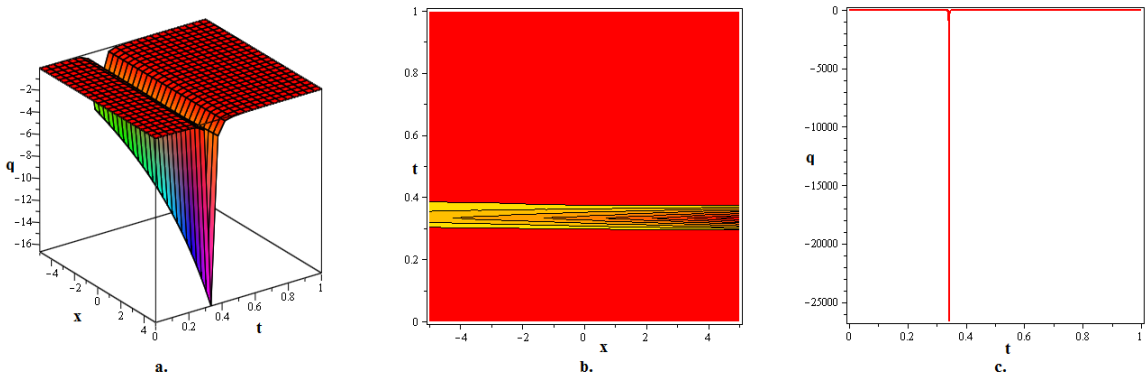

Figure 9. a. 3D graph, b. contour graph, and c. 2D graph representing optical dark-hump soliton solution $q_{1,11}(t,x)$ articulated in (3.19) for $\lambda := 4, \eta := 2, \nu := 0, \varpi := 2, h := 2, S_0 := 0.3E^{-2}, \delta := 1, \mu := -1$.

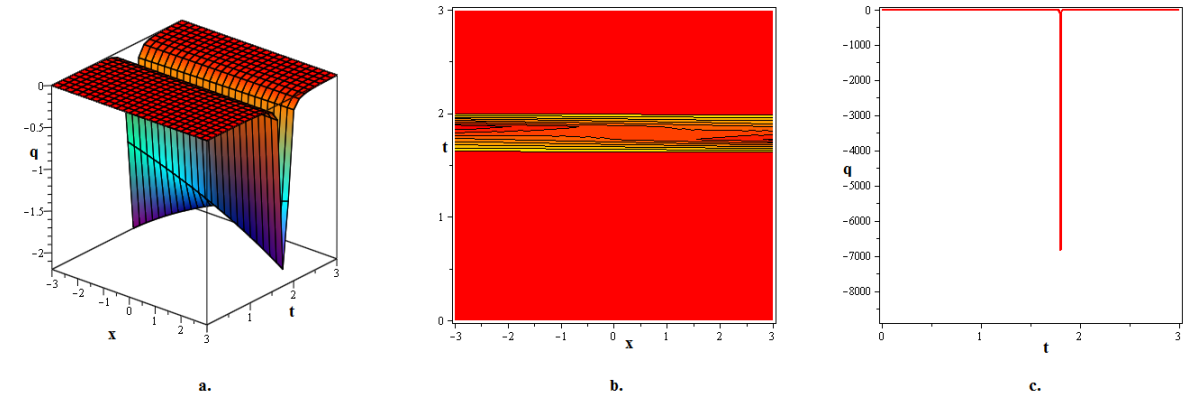

Figure 10. a. 3D graph, b. contour graph, and c. 2D graph representing optical dark-hump soliton solution $q_{2,1}(t,x)$ articulated in (3.20) for $\lambda := 1, \eta := 1, \nu := 1, F_1 := 0.3E^{-2}, \delta := 1, \mu := -1$.

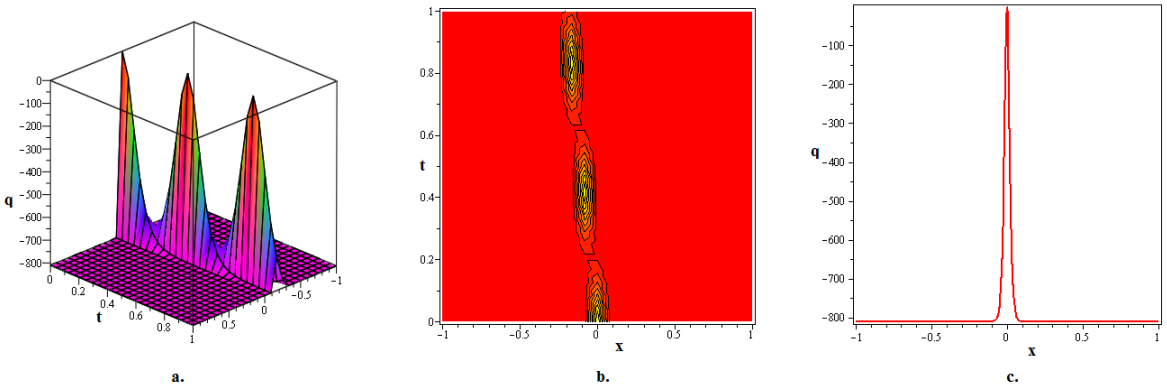

Figure 11. a. 3D graph, b. contour graph, and c. 2D graph representing optical multiple bright-hump soliton solution $q_{2,5}(t,x)$ articulated in (3.24) for $\lambda := 4, \eta := 10, \nu := 4, F_1 := 15, \delta := 3, \mu := -1$.

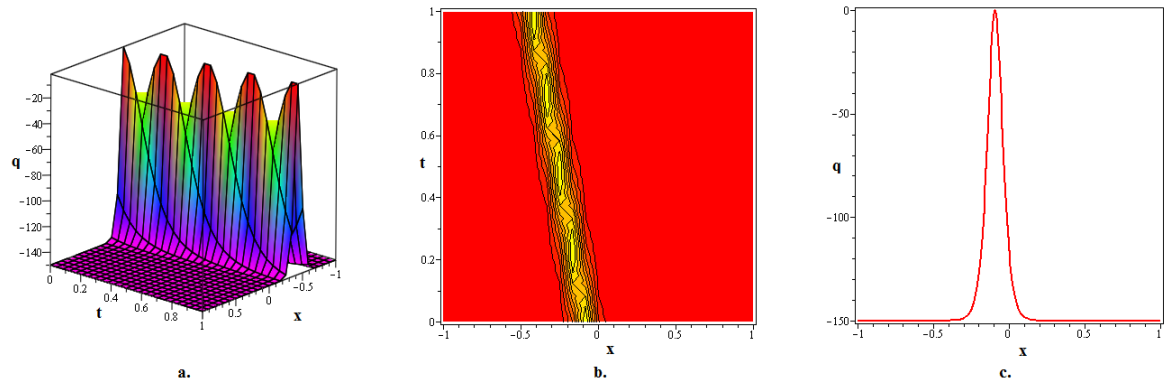

Figure 12. a. 3D graph, b. contour graph, and c. 2D graph representing optical multiple bright-hump soliton solution $q_{2,13}(t,x)$ articulated in (3.32) for $\lambda := 0, \eta := 1, \nu := 2, F_1 := 30, \delta := 5, \mu := -1, b_2 := 5$.

5. Conclusions

In this study, we have generated some precise optical soliton solutions for K-IIS by using the effective RMESEM. We were able to find solutions that were trigonometric, rational, hyperbolic, exponential, and hyperbolic. To aid in your understanding of the propagation behaviors of the generated optical solitons, we have provided extra 3D, contour, and 2D charts for the free selections of the physical parameters. The obtained solitons solutions take the form of fractals due to the instability caused by periodic-axial perturbation in complex solutions, whereas the real solutions, within the context of K-IIS, take the form of hump solitons, as these visuals demonstrate the graphic behaviors of several optical solitons. In the telecom sector, the generated optical solitons have a number of useful applications. By extending the spectrum of optical soliton solutions, offering insightful information on the K-IIS dynamics, and suggesting possible applications in nonlinear model management, our recruited RMESEM further demonstrates its value. Although the RMESEM has greatly advanced our knowledge of soliton dynamics and how they relate to the models that are being studied, it is crucial to recognize the limits of this approach, especially in situations where the nonlinear component and largest derivative are not equally balanced. Despite this drawback, the current study shows that the technique used in this work is highly productive, trustworthy, and adaptable for nonlinear issues in a range of natural scientific fields. Further research on the soliton's stability, fractal solitons' sensitivity, the inclusion of fractional derivatives and their effects on fractal solitons, and the computation of fractal theory's scaling factors are the future's goals of this project.

Motivated by our findings, we anticipate that further trials will validate the soliton formations we have estimated, including the fascinating fractal structures, determined by our analysis of the K-IIS. We anticipate that similar motifs with hump solitons may manifest in optical studies, in which solitons have already been detected, particularly if axial-periodic perturbations are used. Our contour, 2D, and 3D representations make it easy to recognize these formations, and our hypothesis may be confirmed by comparable practical configurations. This work paves the way for valuable experimental confirmation in optical structures while also improving our theoretical understanding of theory.

Author contributions

Azzh Saad Alshehry: conceptualization, formal analysis, investigation, methodology, project administration, supervision, validation, writing-original draft, writing-review and editing; Safyan Mukhtar: data curation, investigation, software, visualization, writing-original draft; Ali M. Mahnashi: formal analysis, methodology, investigation, software, supervision, validation. All authors have read and approved the final version of the manuscript for publication.

Acknowledgments

This work was supported by Princess Nourah bint Abdulrahman University Researchers Supporting Project number (PNURSP2024R183), Princess Nourah bint Abdulrahman University, Riyadh, Saudi Arabia. This work was supported by the Deanship of Scientific Research, Vice Presidency for Graduate Studies and Scientific Research, King Faisal University, Saudi Arabia (KFU241810).

Funding

This work was supported by Princess Nourah bint Abdulrahman University Researchers Supporting Project number (PNURSP2024R183), Princess Nourah bint Abdulrahman University, Riyadh, Saudi Arabia. This work was supported by the Deanship of Scientific Research, Vice Presidency for Graduate Studies and Scientific Research, King Faisal University, Saudi Arabia (KFU241810).

Conflict of interest

The authors declare that they have no conflicts of interest.

References

1. W. Gao, H. Rezazadeh, Z. Pinar, H. M. Baskonus, S. Sarwar, G. Yel, Novel explicit solutions for the nonlinear Zoomeron equation by using newly extended direct algebraic technique, *Opt. Quant. Electron.*, **52** (2020), 52. https://doi.org/10.1007/s11082-019-2162-8
2. C. Zhu, M. Al-Dossari, S. Rezapour, B. Gunay, On the exact soliton solutions and different wave structures to the (2+1) dimensional Chaffee-Infante equation, *Results Phys.*, **57** (2024), 107431. https://doi.org/10.1016/j.rinp.2024.107431
3. C. Zhu, M. Al-Dossari, S. Rezapour, S. Shateyi, On the exact soliton solutions and different wave structures to the modified Schrödinger's equation, *Results Phys.*, **54** (2023), 107037. https://doi.org/10.1016/j.rinp.2023.107037
4. C. Zhu, S. A. Idris, M. E. M. Abdalla, S. Rezapour, S. Shateyi, B. Gunay, Analytical study of nonlinear models using a modified Schrödinger's equation and logarithmic transformation, *Results Phys.*, **55** (2023), 107183. https://doi.org/10.1016/j.rinp.2023.107183
5. M. Alqudah, S. Mukhtar, H. A. Alyousef, S. M. Ismaeel, S. A. El-Tantawy, F. Ghani, Probing the diversity of soliton phenomena within conformable Estevez-Mansfield-Clarkson equation in shallow water, *AIMS Math.*, **9** (2024), 21212–21238. https://doi.org/10.3934/math.20241030
6. M. Ghasemi, High order approximations using spline-based differential quadrature method: implementation to the multi-dimensional PDEs, *Appl. Math. Model.*, **46** (2017), 63–80. https://doi.org/10.1016/j.apm.2017.01.052
7. N. Perrone, R. Kao, A general finite difference method for arbitrary meshes, *Comput. Struct.*, **5** (1975), 45–57. https://doi.org/10.1016/0045-7949(75)90018-8
8. S. Mahmood, R. Shah, H. Khan, M. Arif, Laplace adomian decomposition method for multi dimensional time fractional model of Navier-Stokes equation, *Symmetry*, **11** (2019), 149. https://doi.org/10.3390/sym11020149
9. M. A. Abdou, A. A. Soliman, New applications of variational iteration method, *Phys. D*, **211** (2005), 1–8. https://doi.org/10.1016/j.physd.2005.08.002
10. O. C. Zienkiewicz, R. L. Taylor, J. Z. Zhu, *The finite element method: its basis and fundamentals*, 6 Eds., Elsevier, 2005.

11. M. M. A. Hammad, R. Shah, B. M. Alotaibi, M. Alotiby, C. G. L. Tiofack, A. W. Alrowaily, et al., On the modified versions of $(\frac{G'}{G})$-expansion technique for analyzing the fractional coupled Higgs system, *AIP Adv.*, **13** (2023), 105131. https://doi.org/10.1063/5.0167916

12. Y. Chen, B. Li, H. Zhang, Generalized Riccati equation expansion method and its application to the Bogoyavlenskii's generalized breaking soliton equation, *Chin. Phys.*, **12** (2003), 940. https://doi.org/10.1088/1009-1963/12/9/303

13. E. Yusufoğlu, A. Bekir, Solitons and periodic solutions of coupled nonlinear evolution equations by using the sine-cosine method, *Int. J. Comput. Math.*, **83** (2006), 915–924. https://doi.org/10.1080/00207160601138756

14. H. Liu, T. Zhang, A note on the improved $\tan(\phi(\xi)/2)$-expansion method, *Optik*, **131** (2017), 273–278. https://doi.org/10.1016/j.ijleo.2016.11.029

15. M. Kaplan, A. Bekir, A. Akbulut, E. Aksoy, The modified simple equation method for nonlinear fractional differential equations, *Rom. J. Phys.*, **60** (2015), 1374–1383.

16. M. Guo, H. Dong, J. Liu, H. Yang, The time-fractional mZK equation for gravity solitary waves and solutions using sech-tanh and radial basic function method, *Nonlinear Anal.*, **24** (2019), 1–19. https://doi.org/10.15388/NA.2019.1.1

17. S. Meng, F. Meng, F. Zhang, Q. Li, Y. Zhang, A. Zemouche, Observer design method for nonlinear generalized systems with nonlinear algebraic constraints with applications, *Automatica*, **162** (2024), 111512. https://doi.org/10.1016/j.automatica.2024.111512

18. M. Lei, H. Liao, S. Wang, H. Zhou, J. Zhu, H. Wan, et al., Electro-sorting create heterogeneity: constructing a multifunctional Janus film with integrated compositional and microstructural gradients for guided bone regeneration, *Adv. Sci.*, **11** (2024), 2307606. https://doi.org/10.1002/advs.202307606

19. R. Ali, M. M. Alam, S. Barak, Exploring chaotic behavior of optical solitons in complex structured conformable perturbed Radhakrishnan-Kundu-Lakshmanan model, *Phys. Scr.*, **99** (2024), 095209. https://doi.org/10.1088/1402-4896/ad67b1

20. R. Ali, A. S. Hendy, M. R. Ali, A. M. Hassan, F. A. Awwad, E. A. Ismail, Exploring propagating soliton solutions for the fractional Kudryashov-Sinelshchikov equation in a mixture of liquid-gas bubbles under the consideration of heat transfer and viscosity, *Fractal Fract.*, **7** (2023), 773. https://doi.org/10.3390/fractalfract7110773

21. X. Xie, Y. Gao, F. Hou, T. Cheng, A. Hao, H. Qin, Fluid inverse volumetric modeling and applications from surface motion, *IEEE Trans. Vis. Comput. Gr.*, 2024, 1–17. https://doi.org/10.1109/TVCG.2024.3370551

22. J. Hong, L. Gui, J. Cao, Analysis and experimental verification of the tangential force effect on electromagnetic vibration of PM motor, *IEEE Trans. Energy Conver.*, **38** (2023), 1893–1902. https://doi.org/10.1109/TEC.2023.3241082

23. S. Y. Arafat, S. M. Rayhanul Islam, Bifurcation analysis and soliton structures of the truncated M-fractional Kuralay-II equation with two analytical techniques, *Alex. Eng. J.*, **105** (2024), 70–87. https://doi.org/10.1016/j.aej.2024.06.079

24. G. Zhang, W. Li, M. Yu, H. Huang, Y. Wang, Z. Han, et al., Electric-field-driven printed 3D highly ordered microstructure with cell feature size promotes the maturation of engineered cardiac tissues, *Adv. Sci.*, **10** (2023), 2206264. https://doi.org/10.1002/advs.202206264
25. S. M. Rayhanul Islam, Bifurcation analysis and soliton solutions to the doubly dispersive equation in elastic inhomogeneous Murnaghans rod, *Sci. Rep.*, **14** (2024), 11428. https://doi.org/10.1038/s41598-024-62113-z
26. Y. Kai, Z. Yin, On the Gaussian traveling wave solution to a special kind of Schrodinger equation with logarithmic nonlinearity, *Mod. Phys. Lett. B*, **36** (2021), 2150543. https://doi.org/10.1142/S0217984921505436
27. Y. Kai, J. Ji, Z. Yin, Study of the generalization of regularized long-wave equation, *Nonlinear Dyn.*, **107** (2022), 2745–2752. https://doi.org/10.1007/s11071-021-07115-6
28. Y., Kai, Z. Yin, Linear structure and soliton molecules of Sharma-Tasso-Olver-Burgers equation, *Phys. Lett. A*, **452** (2022), 128430. https://doi.org/10.1016/j.physleta.2022.128430
29. H. Tian, M. Zhao, J. Liu, Q. Wang, X. Yu, Z. Wang, Dynamic analysis and sliding mode synchronization control of chaotic systems with conditional symmetric fractional-order memristors, *Fractal Fract.*, **8** (2024), 307. https://doi.org/10.3390/fractalfract8060307
30. L. Liu, S. Zhang, L. Zhang, G. Pan, J. Yu, Multi-UUV maneuvering counter-game for dynamic target scenario based on fractional-order recurrent neural network, *IEEE Trans. Cybernetics*, **53** (2023), 4015–4028. https://doi.org/10.1109/TCYB.2022.3225106
31. M. Li, T. Wang, F. Chu, Q. Han, Z. Qin, M. J. Zuo, Scaling-basis chirplet transform, *IEEE Trans. Ind. Electron.*, **68** (2021), 8777–8788. https://doi.org/10.1109/TIE.2020.3013537
32. R. Ali, S. Barak, A. Altalbe, Analytical study of soliton dynamics in the realm of fractional extended shallow water wave equations, *Phys. Scr.*, **99** (2024), 065235. https://doi.org/10.1088/1402-4896/ad4784
33. A. Iftikhar, A. Ghafoor, T. Zubair, S. Firdous, S. T. Mohyud-Din, Solutions of (2 + 1) dimensional generalized KdV, Sin Gordon and Landau-Ginzburg-Higgs equations, *Sci. Res. Essays*, **8** (2013), 1349–1359.
34. M. M. Bhatti, D. Q. Lu, An application of Nwogu's Boussinesq model to analyze the head-on collision process between hydroelastic solitary waves, *Open Phys.*, **17** (2019), 177–191. https://doi.org/10.1515/phys-2019-0018
35. J. H., He, X. H. Wu, Exp-function method for nonlinear wave equations, *Chaos Soliton. Fract.*, **30** (2006), 700–708. https://doi.org/10.1016/j.chaos.2006.03.020
36. S. Behera, N. H. Aljahdaly, Nonlinear evolution equations and their traveling wave solutions in fluid media by modified analytical method, *Pramana*, **97** (2023), 130. https://doi.org/10.1007/s12043-023-02602-4
37. H. Khan, S. Barak, P. Kumam, M. Arif, Analytical solutions of fractional Klein-Gordon and gas dynamics equations, via the (G'/G)-expansion method, *Symmetry*, **11** (2019), 566. https://doi.org/10.3390/sym11040566
38. W. Thadee, A. Chankaew, S. Phoosree, Effects of wave solutions on shallow-water equation, optical-fibre equation and electric-circuit equation, *Maejo Int. J. Sci. Tech.*, **16** (2022), 262–274.

39. A. R. Alharbi, M. B. Almatrafi, Riccati-Bernoulli sub-ODE approach on the partial differential equations and applications, *Int. J. Math. Comput. Sci.*, **15** (2020), 367–388.

40. M. Cinar, A. Secer, M. Ozisik, M. Bayram, Derivation of optical solitons of dimensionless Fokas-Lenells equation with perturbation term using Sardar sub-equation method, *Opt. Quant. Electron.*, **54** (2022), 402. https://doi.org/10.1007/s11082-022-03819-0

41. J. F. Alzaidy, Fractional sub-equation method and its applications to the space-time fractional differential equations in mathematical physics, *Br. J. Math. Comput. Sci.*, **3** (2013), 153–163.

42. M. M. Al-Sawalha, H. Yasmin, R. Shah, A. H. Ganie, K. Moaddy, Unraveling the dynamics of singular stochastic solitons in stochastic fractional Kuramoto-Sivashinsky equation, *Fractal Fract.*, **7** (2023), 753. https://doi.org/10.3390/fractalfract7100753

43. H. Yasmin, N. H. Aljahdaly, A. M. Saeed, R. Shah, Probing families of optical soliton solutions in fractional perturbed Radhakrishnan-Kundu-Lakshmanan model with improved versions of extended direct algebraic method, *Fractal Fract.*, **7** (2023), 512. https://doi.org/10.3390/fractalfract7070512

44. M. Aldandani, A. A. Altherwi, M. M. Abushaega, Propagation patterns of dromion and other solitons in nonlinear Phi-Four (ϕ^4) equation, *AIMS Math.*, **9** (2024), 19786–19811. https://doi.org/10.3934/math.2024966

45. N. Iqbal, M. B. Riaz, M. Alesemi, T. S. Hassan, A. M. Mahnashi, A. Shafee, Reliable analysis for obtaining exact soliton solutions of (2 + 1)-dimensional Chaffee-Infante equation, *AIMS Math.*, **9** (2024), 16666–16686. https://doi.org/10.3934/math.2024808

46. K. J. Wang, F. Shi, Multi-soliton solutions and soliton molecules of the (2 + 1)-dimensional Boiti-Leon-Manna-Pempinelli equation for the incompressible fluid, *Europhys. Lett.*, **145** (2024), 42001. https://doi.org/10.1209/0295-5075/ad219d

47. W. Alhejaili, E. Az-Zo'bi, R. Shah, S. A. El-Tantawy, On the analytical soliton approximations to fractional forced Korteweg-de Vries equation arising in fluids and plasmas using two novel techniques, *Commun. Theor. Phys.*, **76** (2024), 085001. https://doi.org/10.1088/1572-9494/ad53bc

48. S. Noor, W. Albalawi, R. Shah, M. M. Al-Sawalha, S. M. Ismaeel, S. A. El-Tantawy, On the approximations to fractional nonlinear damped Burger's-type equations that arise in fluids and plasmas using Aboodh residual power series and Aboodh transform iteration methods, *Front. Phys.*, **12** (2024), 1374481. https://doi.org/10.3389/fphy.2024.1374481

49. S. Noor, W. Albalawi, R. Shah, A. Shafee, S. M. Ismaeel, S. A. El-Tantawy, A comparative analytical investigation for some linear and nonlinear time-fractional partial differential equations in the framework of the Aboodh transformation, *Front. Phys.*, **12** (2024) 1374049. https://doi.org/10.3389/fphy.2024.1374049

50. H. Yasmin, A. S. Alshehry, A. H. Ganie, A. M. Mahnashi, R. Shah, Perturbed Gerdjikov-Ivanov equation: soliton solutions via Backlund transformation, *Optik*, **298** (2024), 171576. https://doi.org/10.1016/j.ijleo.2023.171576

51. S. Alshammari, K. Moaddy, R. Shah, M. Alshammari, Z. Alsheekhhussain, M. M. Al-Sawalha, et al., Analysis of solitary wave solutions in the fractional-order Kundu-Eckhaus system, *Sci. Rep.*, **14** (2024), 3688. https://doi.org/10.1038/s41598-024-53330-7

52. C. Zhu, M. Al-Dossari, S. Rezapour, S. Shateyi, B. Gunay, Analytical optical solutions to the nonlinear Zakharov system via logarithmic transformation, *Results Phys.*, **56** (2024), 107298. https://doi.org/10.1016/j.rinp.2023.107298

53. X. Xi, J. Li, Z. Wang, H. Tian, R. Yang, The effect of high-order interactions on the functional brain networks of boys with ADHD, *Eur. Phys. J. Spec. Top.*, **233** (2024), 817–829. https://doi.org/10.1140/epjs/s11734-024-01161-y

54. Z. Wang, M. Chen, X. Xi, H. Tian, R. Yang, Multi-chimera states in a higher order network of FitzHugh-Nagumo oscillators, *Eur. Phys. J. Spec. Top.*, **233** (2024), 779–786. https://doi.org/10.1140/epjs/s11734-024-01143-0

55. M. Lakshmanan, Continuum spin system as an exactly solvable dynamical system, *Phys. Lett. A*, **61** (1977), 53–54. https://doi.org/10.1016/0375-9601(77)90262-6

56. V. E. Zakharov, L. A. Takhtadzhyan, Equivalence of the nonlinear Schrödinger equation and the equation of a Heisenberg ferromagnet, *Theor. Math. Phys.*, **38** (1979), 17–23.

57. Z. Sagidullayeva, G. Nugmanova, R. Myrzakulov, N. Serikbayev, Integrable Kuralay equations: geometry, solutions and generalizations, *Symmetry*, **14** (2022), 1374. https://doi.org/10.3390/sym14071374

58. W. A. Faridi, M. A. Bakar, Z. Myrzakulova, R. Myrzakulov, A. Akgul, S. M. El Din, The formation of solitary wave solutions and their propagation for Kuralay equation, *Results Phys.*, **52** (2023), 106774. https://doi.org/10.1016/j.rinp.2023.106774

59. T. Mathanaranjan, Optical soliton, linear stability analysis and conservation laws via multipliers to the integrable Kuralay equation, *Optik*, **290** (2023), 171266. https://doi.org/10.1016/j.ijleo.2023.171266

60. A. Zafar, M. Raheel, M. R. Ali, Z. Myrzakulova, A. Bekir, R. Myrzakulov, Exact solutions of M-fractional Kuralay equation via three analytical schemes, *Symmetry*, **15** (2023), 1862. https://doi.org/10.3390/sym15101862

61. A. Farooq, W. X. Ma, M. I. Khan, Exploring exact solitary wave solutions of Kuralay-II equation based on the truncated M-fractional derivative using the Jacobi elliptic function expansion method, *Opt. Quant. Electron.*, **56** (2024), 1105. https://doi.org/10.1007/s11082-024-06841-6

62. Y. Xiao, S. Barak, M. Hleili, K. Shah, Exploring the dynamical behaviour of optical solitons in integrable Kairat-II and Kairat-X equations, *Phys. Scr.*, **99** (2024), 095261. https://doi.org/10.1088/1402-4896/ad6e34

AIMS Press